IEEE Access
Multidisciplinary | Rapid Review | Open Access Journal

Received October 8, 2018, accepted October 29, 2018, date of publication November 15, 2018,
date of current version December 27, 2018.

Digital Object Identifier 10.1109/ACCESS.2018.2879338

Intra-Frame Error Concealment Scheme Using 3D Reversible Data Hiding in Mobile Cloud Environment

YAN LI CHEN[1,2], HONGXIA WANG[3], YI HU[4], AND ASAD MALIK[1]
[1]School of Information Science and Technology, Southwest Jiaotong University, Chengdu 611756, China
[2]School of Engineering, Tibet University, Lhasa 850000, China
[3]College of Cybersecurity, Sichuan University, Chengdu 610065, China
[4]Computer Science Department, Northern Kentucky University, Highland Heights, KY 41099, USA

Corresponding author: Hongxia Wang (hxwang@scu.edu.cn)

This work was supported by the National Natural Science Foundation of China (NSFC) under Grant U1536110.

ABSTRACT In mobile cloud environment, data are mainly transmitted via wireless noisy channels, which may result in random transmission errors (RTE) with a high probability. For video transmission, noisy channels may cause significant degradation of the content. Improving or keeping video quality over lossy channel is, therefore, a very important research topic. Error concealment with data hiding (ECDH) is an effective way to conceal the errors introduced by channels, and it can reduce error propagation between neighbor blocks/frames. The existing video ECDH methods often embed the motion vectors (MVs) into the specific locations. Nevertheless, specific embedding locations cannot resist against RTE. To compensate the RTE in mobile cloud environment, we propose a video ECDH scheme using 3D reversible data hiding (RDH), in which we create multiple duplicate copies of each MV to improve the robustness of the ECDH scheme. Furthermore, all the duplicate copies and original MVs are embedded into macroblocks randomly. However, embedding more data would make quality of marked video decreased. In addition, satisfactory trade-off between the introduced distortion and the reconstructed video quality can be achieved by tuning the number of duplicate copies. For random embedding, the lost probability of the MVs decreases rapidly which can result in better error concealment performance. Experimental results show that the peak signal to noise ratio values gain about 5 dB at least comparing with the existing ECDH methods. Meanwhile, the proposed method improves the video quality significantly.

INDEX TERMS Video error concealment, 3D RDH, Mobile cloud, Random embedding.

I. INTRODUCTION

With rapid growth of information and communication technology, multimedia is becoming the popular format in the Internet. However, the storage space, computer resource, and bandwidth limit the development of multimedia communication. Cloud computing moves services, computation, and data to location-transparent centralized facilities or providers to solve these problems [1].

The cloud services are becoming more and more popular, especially in computing and storage aspects. Now, many multimedia companies have cloud-based platforms or shift their storage and computing services to the third parties, e.g., Youtube, Dailymotion, Tencent, and iQiYi [2]. Often services can be provided with lower cost and simpler architecture. In this case, with the development of terminal equipment, mobile cloud becomes a popular environment.

Currently, video quality is becoming more important, especially for the medical video, surveillance video. To guarantee better video services, mobile cloud provides efficient platform for computing, storage and transmission. Since there is massive redundancy in the video sequence, they always need to be compressed before storing and transmitting. The popular video compression standard such as MPEG-2/4, H.264/AVC, and H.265 demands either parallel or distributed processing platform [2], which exists in cloud environment. In the case of cloud computing, many video service providers (VSPs) rent out the distribution architecture from cloud service providers (CSPs) [3].

Since video is a visual media, the quality is an important factor. However, in mobile cloud environment, the video transmission encounters challenges [2]. Firstly, since both the low and high speed networks exist in the Internet, it may

cause data buffering at different locations during data transmission. Then out of order delivery and packet loss or drops may occur. Secondly, some video transmission is based on connectionless protocols, and it cannot provide lossless data transmission. Both the two challenges are caused by channel, and they may lead to random transmission errors (RTE) and have impact on the visual quality of videos.

Beside the channel station, video compression standard is another factor which may influence the video quality. There are two basic encoding modes for video compressing, inter-frame and intra-frame. Usually, macroblocks (MBs) are the basis processing units under intra mode. That is to say, the video quality is mainly based on visual quality of every MB. Error resilience and error concealment are used as popular technologies to improve the video quality, and the error concealment techniques are used to conceal errors at the decoder side especially for the losing packet problem.

There are two methods used for error concealment at the decoder side, the data hiding-based and spatial/temporal correlation-based (data interpolation) methods [1], [4]. The data interpolation method [5], [6], which is based on spatial/temporal correlation, works well in the case of the successfully received data. However, once the errors occurred, the spatial/temporal correlation may be damaged, especially for activity blocks. Conversely, the performance of methods based on data hiding mainly depends on whether the marked data can be extracted and reflects the frames characteristics. The extracted data is used for error concealment, thus, it reduces the relevance between transmission and video sequence.

Data hiding is a popular technique used in the field of multimedia security such as copyright protection, content authentication and secret communication [7]. Because the data hiding has the advantage that the mark data can be carried in a seamless way, it has been employed to conceal video errors produced by the transmission. Adsumilli *et al.* [8] proposed an error concealment technique in which the 2-level discrete wavelet transforms (DWT) approximation coefficients are converted to halftone image which is considered as marked data and embedded into original frame. Yilmaz and Alatan [9] presented an error concealment method using edge orientation information as marked data. Chen *et al.* [4] compressed the residuals of the neighbor frames by compressed sensing (CS) as marked data at the encoder side, and reconstructed the original residual by CS to conceal the channel errors at decoder side.

In general, the more valid information about frame is embedded, the better error concealment performance is. However, embedding more information means to degrade the quality of marked video. So, the goal of data hiding in error concealment scheme is to improve the quality of marked video and provide more information for error concealment. For high correlation between neighbor frames, inter-frame correlation is used to conceal intra-frame errors, and a frame can be recovered from the reference frame and motion vectors (MVs). In existing methods, the MVs are hidden in the quantized discrete cosine transform (QDCT) coefficients to conceal errors at the decoder side [10], [11]. Yao *et al.* [10], the MVs in the region of interest (ROI), which are shared in a frame group, were embedded into the background region within the same frame. Chen *et al.* [11], the MVs of every MB are embedded into the QDCT coefficients of neighboring MBs, and at the decoder side, the extracted MVs are used to find the matching MBs. However, the coefficients which have carried message can not be recovered after data extraction. And also, they embedded data into given MBs, and it cannot resist the random error from channel.

To improve video quality at the decoder side, reversible data hiding (RDH) [12], [13] is used to recover the cover losslessly. Chung *et al.* [14] presented a video error concealment scheme using RDH. Each MV is embedded into QDCT coefficients with zero values of the corresponding MB by a circular embedding scheme. Xu *et al.* [15] proposed a RDH-based intra-frame error concealment method, in which it included MV data pre-processing and the selection of embedding locations. Later, Xu *et al.* [7] raised a two dimensional RDH-based intra-frame error concealment scheme, and it focused on reducing the embedding distortions caused by RDH.

Nevertheless, the error concealment scheme should be improved. Firstly, to resist RTE, the error concealment performance in [14]–[16] cannot benefit from changeless embedding location. Secondly, embedding a MV of the MBs sized 16×16 into a MB is a valuable selection to gain better error concealment performance and reduce the amount of marked data. However, to enhance the robustness of error concealment, more MVs are to be embedded, such as, creating duplicate copies for MVs or MVs with smaller block size are considered as marked data, then higher capacity and lower rate of embedding modification RDH methods are needed. Thirdly, the computational efficiency is a important factor in cloud environment. For 1D and 2D RDH scheme based on histogram shifting [17], every embedding operation only has two or four modification directions to embed one or two bits. However, high dimension RDH, which has more modification directions, can improve the computational efficiency. Also it can improve the embedding capacity and decrease the rate of embedding modification. But the dimension may affect the complexity of data hiding, and there is no evidence to show higher dimension RDH may provide better capacity-distortion performance. So, in order to solve these problems in mobile cloud environment, an intra-frame error concealment scheme using 3D RDH, which can recover the marked data losslessly, is proposed.

In this paper, H.264 [18], [19] is selected as the implementation platform. The rest of this paper is organized as follows. In Section 2, the main idea of 3D RDH is illustrated. The proposed 3D RDH based error concealment method is presented in Section3. In Section 4, experimental results are introduced. At last, the paper is concluded in Section 5.

II. PROPOSED 3D RDH SCHEME

In this paper, data is embedded into the QDCT coefficients, we denote the carrier frame as f, and $f_{i,j}(k)$ denote the *kth* original QDCT coefficient in the *jth* blocks of the *ith* MB. The methods in [14] and [15] focus on using one-dimensional (1D) coefficient histogram for RDH. The 1D RDH is usually defined as

$$h(r) = \natural\{f_{i,j}(k)|f_{i,j}(k) = r\}. \tag{1}$$

where $\natural$ denotes the cardinal number of a set, and r is a specified value of QDCT coefficient. Specifically, by considering every two adjacent residual coefficients together, similar to definition of 1D RDH, 2D RDH is defined as

$$h(r_1, r_2) = \natural\{f_{i,j}(2m), f_{i,j}(2m+1)| \times f_{i,j}(2m) = r_1, f_{i,j}(2m+1) = r_2\}. \tag{2}$$

In 2D RDH, one or two bits are embedded into a pair of QDCT coefficient [20], and the pair can be modified to 2^2 different pairs. if we consider embedding data into triples and using ± 1 embedding, there are 3^3 modification space which contains 6 triple with direct distance of 1. For 3D RDH method, every three adjacent elements are considered as a triple, it is defined as

$$h(r_1, r_2, r_3) = \natural\{(f_{i,j}(3m), f_{i,j}(3m+1), f_{i,j}(2m+3))| f_{i,j}(3m) = r_1, f_{i,j}(3m+1) = r_2, f_{i,j}(3m+2) = r_3\} \tag{3}$$

Since most of the MVs have zero or near-zero values [7], for 1D RDH [14], [15], residual coefficients do not need to be modified [7] to embedding zeros, but the histogram shifting operation for the non-zero coefficients is still to be carried out. For 2D RDH, beside the coordinate (0, 0), half coefficients in a coefficients pair are needed to be modified to embed one/two bits. In [7] and [20], at most two bits are embedded into a coefficient pair, and only one coefficient is modified with ± 1. Therefore, both the 1D RDH and 2D RDH cannot meet the demands of the capacity-distortion performance well.

Recently, a 3D RDH scheme is proposed in [21] to decrease the distortion in video. In [21] at most two bits are embedded into a coefficient triple, and the capacity is not very suitable for our application scenarios. In order to decrease the rate of embedding modification and improve capacity, a 3D RDH based on histogram shifting [22]–[24]with high capacity and low distortion is proposed in this paper. The proposed 3D RDH scheme is shown in Fig.1. It can carry three bits and only need modify at most two QDCT coefficients for a triple, comparing with the 3D RDH in [21], the proposed 3D RDH in this paper improve the capacity and decrease the modification rate.

To illustrate the data hiding produce, assume original carrier is denoted as $F = \{f_1, f_2, \cdots, f_t\}$, $F' = \{f_1', f_2', \cdots, f_t'\}$ denotes the marked carrier, $B = \{b_1, b_2, \cdots, b_s\}$ denote the marked binary string, where f_k and f_k' denote the *kth* triple for original carrier and marked carrier, t is the triple number, s is the length of marked binary string and b_l denote the *lth* binary bit. Assuming from *lth* element in B, 2 or 3 bits are embedded into the *kth* triple of carrier, then, embedding procedure is as follows.

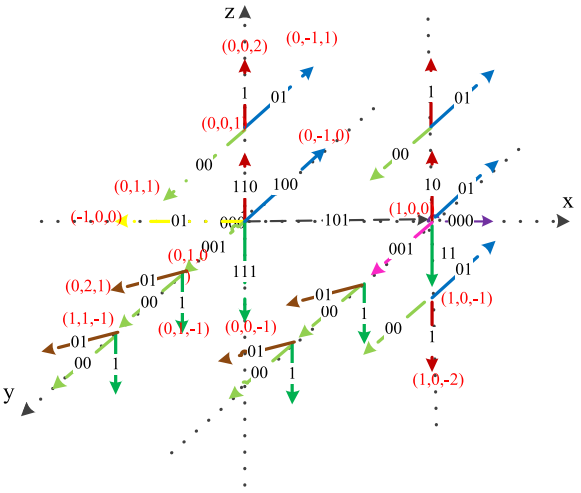

FIGURE 1. Illustration of the proposed 3D reversible data hiding.

(1) If $f_k = (0, 0, 0)$, loacted in the origin in Fig.1, the marked coefficient triple f_k' is determined as follows

$$f_k' = \begin{cases} (0,0,0) & if\ b_l b_{l+1} b_{l+2} = 000 \\ (0,1,0) & if\ b_l b_{l+1} b_{l+2} = 001 \\ (-1,0,0) & if\ b_l b_{l+1} = 01 \\ (0,-1,0) & if\ b_l b_{l+1} b_{l+2} = 100 \\ (1,0,0) & if\ b_l b_{l+1} b_{l+2} = 101 \\ (0,0,1) & if\ b_l b_{l+1} b_{l+2} = 110 \\ (0,0,-1) & if\ b_l b_{l+1} b_{l+2} = 111. \end{cases} \tag{4}$$

In this case, three bits are embedded by modifying one element in a triple at most with the probability 0.75.

(2) If $f_k = (x, 0, z)$, $z \neq 0$, located with coordinates which are the origin of the red arrows in Fig.1, the the marked coefficient triple f_k' is determined as follows

$$f_k' = \begin{cases} (x,1,y) & if\ \ b_l b_{l+1} = 00 \\ (x,-1,y) & if\ \ b_l b_{l+1} = 01 \\ (x,0,y+sign(y)) & if\ \ b_l = 1. \end{cases} \tag{5}$$

where $sign(y)$ denotes the symbol of y. In this case, at least one bit is embedded with modifying one of three coefficients. Comparing with the 3D RDH [21], the capacity-distortion performance is improved.

(3) If $f_k = (x, 0, 0), x \neq 0$, located with coordinates which are the origin of the black arrows in Fig.1, the marked coefficient triple f_k' is determined as follows

$$f_k' = \begin{cases} (x+1,0,0) & if\ b_l b_{l+1} b_{l+2} = 000 \\ (x,1,0) & if\ b_l b_{l+1} b_{l+2} = 001 \\ (x,-1,0) & if\ b_l b_{l+1} = 01. \end{cases} \tag{6}$$

In this case, more than two bits are embedded by ±1. However, in the 3D RDH [21], only one bit can be embedded with the same distortion.

(4) If $f_k = (x, y, 0), x \neq 0, y \neq 0$, located with coordinates which are the origin of the green and brown arrows in Fig.1 the marked coefficient triple f_k' is determined as follows

$$f_k' = \begin{cases} (x, y + sign(y), 0) & if \;\; b_l b_{l+1} = 00 \\ (x, y + sign(y), 1) & if \;\; b_l b_{l+1} = 01 \\ (x, y, -1) & if \;\; b_l = 1. \end{cases} \tag{7}$$

In this case, one or two bits are embedded with modifying one coefficient. For the large quantization step, most of the AC coefficients are zeros. This case is occurred with low probability infrequently.

(5) If $f_k = (x, y, z), x, y, z \in Z$, and $y > 0, z \neq 0$, the coefficient triple f_k' is shifted as follows.

$$f_k' = (x, y + 1, z + sign(z)) \tag{8}$$

(6) If $f_k = (x, y, z), x, y, z \in Z$, and $y < 0$ and $z \neq 0$, the coefficient triple f_k' is shifted as follows.

$$f_k' = (x, y - 1, z + sign(z)) \tag{9}$$

In the case 5) and 6), all the shifting are realized by modifying two coefficients in a triple.

Correspondingly, data extraction procedure is an inverse operation of embedding. Similar to the embedding produce, assuming the triple of recovered carrier is $F'' = \{f_1'', f_2'', \cdots, f_t''\}$, and f_k'' is the *kth* recovered triple, *bs* is the extracted binary string from a triple. The extraction produre is described as follows.

(1) If the marked coefficients triple belongs to $f_k' \in \{(0, 0, 0), (1, 0, 0), (0, 1, 0), (0, 0, 1), (-1, 0, 0), (0, -1, 0), (0, 0, -1)\}$, the hidden bits can be extracted as

$$bs = \begin{cases} 000 & if \; f_{=}'(0, 0, 0) \\ 001 & if \; f_k' = (0, 1, 0) \\ 01 & if \; f_k' = (-1, 0, 0) \\ 100 & if \; f_k' = (0, -1, 0) \\ 110 & if \; f_k' = (0, 0, 1) \\ 111 & if \; f_k' = (0, 0, -1). \end{cases} \tag{10}$$

After the bits are extracted, the recovered coefficients triple F'' recovers to (0,0,0).

(2) If the marked coefficients triple $f_k' \in \{\{(x, 0, z)||z| > 1\}, \{(x, 1, z)||z| > 0\}, \{(x, -1, z)||z| > 0\}\}$, the hidden bits are extracted as follows.

$$bs = \begin{cases} 00, & if \; f_k' \in \{(x, 1, z)||z| > 0\} \\ 01, & if \; f_k' \in \{(x, -1, z)||z| > 0\} \\ 1, & if \; f_k' \in \{(x, 0, z)||z| > 1\}. \end{cases} \tag{11}$$

After the bits are extracted, the host coefficient triples are recovered as

$$f_k'' = \begin{cases} (x, 0, z - sign(z)), & if \; f_k'\{(x, 0, z)||z| > 1\} \\ (x, 0, z), & other. \end{cases} \tag{12}$$

(3) If the marked coefficients triple $f_k' \in \{\{(x, 0, 0)||x| > 1\}, \{(x, 0, 1)|x \neq 0\}, \{(x, 0, -1)|x \neq 0\}, \{(x, 1, 0)|x \neq 0\}, \{(x, -1, 0)|x \neq 0\}\}$, the hidden bits are extracted as

$$bs = \begin{cases} 000, & if \; f_k' \in \{(x, 0, 0)||x| > 1\} \\ 001, & if \; f_k' \in \{(x, 1, 0)|x \neq 0\} \\ 01\,, & if \; f_k' \in \{(x, -1, 0)|x \neq 0\} \\ 10\,, & if \; f_k' \in \{(x, 0, 1)|x \neq 0\} \\ 11\,, & if \; f_k' \in \{(x, 0, -1)|x \neq 0\}. \end{cases} \tag{13}$$

After the bits are extracted, the host coefficient triples are recovered as

$$f_k'' = \begin{cases} (x - sign(x), 0, 0), & if \; f_k' \in \{(x, 0, 0)||x| > 1\} \\ (x, 0, 0), & others. \end{cases} \tag{14}$$

(4) If the marked coefficients triple $f_k' \in \{\{(x, y, 0)||y| > 1\}, \{(x, y, 1)||y| > 1\}, \{(x, y, -1)||y| > 0\}\}$, the hidden bits are extracted as

$$bs = \begin{cases} 00, & if \; f_k' \in \{(x, y, 0)||y| > 1\} \\ 01, & if \; f_k' \in \{(x, y, 1)||y| > 1\} \\ 1\,, & if \; f_k' \in \{(x, y, -1)||y| > 0\}. \end{cases} \tag{15}$$

After the bits are extracted, the host coefficient triples are recovered as

$$f_k'' = \begin{cases} (x, y, 0), & if \; f_k'' \in \{(x, y, -1)||y| > 0\} \\ (x, y - sign(y), 0), & others. \end{cases} \tag{16}$$

(5) If the marked coefficient triples belong to shifting triples, they are recovered by inverse-processing of shifting.

If there is no errors through transmission, the QDCT coefficients remain unchanged, then the decoded coefficient triples are equal to the marked triples at the encoder side, and F'' is equal to the original carrier F. If there are errors through transmission, there would be error bits in the extracted binary string. The performance of proposed 3D RDH in this paper is explained in the Section 4.

III. PROPOSED ERROR CONCEALMENT SCHEME

For intra-frame error concealment method, it mainly focuses on the corrupted blocks, and the inter-frame error concealment method focuses on the whole frame errors, such as frame deletion, frame insertion, wrongly ordered frames, and so on. In this scheme, we pay our attentions on corrupted blocks in a frame utilizing inter-frame correlation which is reflected by MVs. In this section, an intra-frame error concealment scheme using proposed 3D RDH is introduced. In this scheme, MVs are embedded in the QDCT coefficients to conceal the intra errors.

A. MARKED DATA GENERATION

1) MARKED DATA

The schemes in [7], [14], and [15] selected the MVs of 16 × 16 MBs as the marked data. In this paper, MVs are

selected as marked data too. However, to improve the robustness of error concealment, multiple duplicate copies of the MVs are created as marked data.

For a MB with size 16 × 16, if the search range is 15, the total number of information bits to be embedded [7] into a MB is :

$$L_{16} = 2(\lceil log_2(215 + 1)\rceil) = 10 \tag{17}$$

where $\lceil\cdot\rceil$ denotes the ceiling function. In this paper, to make more MVs be extracted correctly, at the encoder side, multiple duplicate copies of all the MVs in a frame are created, and all the duplicate copies and their original MVs are considered as marked data. For every MV, assuming $\alpha - 1$ duplicate copies are created, thus, there are α MVs for a MB, and the total number of information bits to be embedded into one MB is:

$$L = \alpha \cdot L_{16} \tag{18}$$

Thus, the larger the α, the higher the capacity in RDH scheme. The embedding capacity is controllable by tuning α. The value of α is related to the number of duplicate MVs for a specific MB, which can improve the quality of the received video. Actually, for videos with different quality demands, the value of α may be different and it is decided by the video owners and receivers.

2) EMBEDDING LOCATIONS

In [7], [14], and [15], the MV of every MB is embedded into the neighbor MB. Actually, errors may be spread into multiple neighbor blocks with a high probability. It is difficult to resist RTEs for the stationary embedding locations.

To keep consistent with the random channel, all the original MVs and their duplicate copies are scrambled randomly with a key(the key is published by video owner), then every α MVs are considered as a group and embedded into MB sequentially. In other words, the α MVs belonging to the specific MB may be distributed in β, $\beta \leq \alpha$ different MBs randomly. And for a lost MB, it can be concealed even if only one duplicate copy of MVs is embedded into the non-corrupted MB. Moreover, The MV of a MBs and all their duplicate copies are lost at the same time with a much low probability.

In order to illustrate the performance of random embedding MVs further, let's assume that there are N blocks in a frame, and the PLR is p. For a specified MB denoted as B, it is lost with probability p. Since the duplicate copies and original MV are scrambled randomly, the α MVs belonging to the specified MB may be embedded into $\beta(\beta = 1, 2, \cdots, \alpha)$ MBs. If we do not consider the impact from embedding of other MVs, the α MVs are embedded into β MBs with probability $P_\beta = \binom{N}{\beta} / \sum_{j=1}^{\alpha} \binom{N}{\beta}$. In the embedding process, the worst condition is $\beta = 1$. If the β host MBs are corrupted at the same time, MB B cannot be concealed correctly and it occurs with probability $P_{nc} = \sum_{\beta=1}^{\alpha} P_\beta \cdot p^\beta$, and it is also the probability that a MB cannot be concealed correctly. Conversely, for a lost MB, even if only one of its α MVs is extracted correctly, MB B can be concealed. So a lost MB can be concealed with the probability $P_c = 1 - P_{nc}$. Obviously, under the normal channel, $p < 0.5$, the relationship between P_c and P_{nc} is described as

$$P_c = 1 - P_{nc} > P_{nc} \tag{19}$$

For random embedding, the relationship between host MBs and the embedding locations of their MVs is changeable. Fig.2 and Fig.3 shows the mapping of host MBs and carrier MBs of the residual coefficients frame in video hall with $\alpha = 1$ and $\alpha = 5$, and it shows the neighbor MBs in the left(the original host MBs) are scrambled dispersedly in the right residual coefficients frame (scrambled embedding locations).

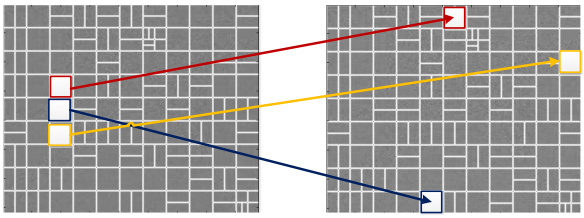

FIGURE 2. The mapping of host MB and scrambled MVs with $\alpha = 1$.

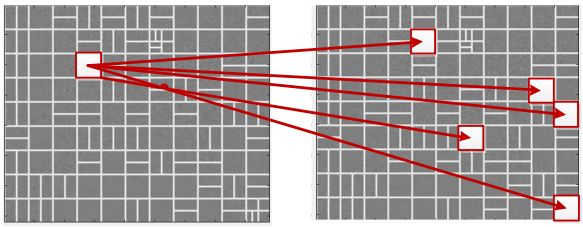

FIGURE 3. The mapping of host MB and scrambled MVs with $\alpha = 5$.

In order to show the impact of random embedding on concealment performance significantly, in this paper, all the pixel values in corrupted MBs that cannot be concealed correctly are set to be zeros and all concealment experimental results in this paper are implemented under this case. In the other words, if the MBs and their MVs are lost at the same time, the decoded MBs are substituted by black blocks. To reveal the impact from random embedding on the concealment performance, Fig.4 shows the comparison of PSNR velues for concealed frames between the random embedding and changeless embedding with PLR 0.1, 0.3 and $\alpha = 1$. We can see from Fig.4 that random embedding has better performance.

B. DATA HIDING AND EXTRACTION

The data hiding and extraction are based on the H.264 encoding/decoding procedure, Fig.5 shows the encoder frame [18], [19], and the decoder is inverse. Considering the video compression process, marked data is embedded into the QDCT coefficients X, and considering the embedding capacity, AC

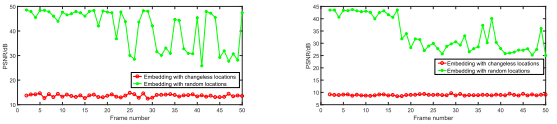

FIGURE 4. PSNR of concealed video sequences foreman with different PLR: (a) PLR=0.1 ;(b) PLR=0.3. (a) PLR=0.1. (b) PLR=0.3.

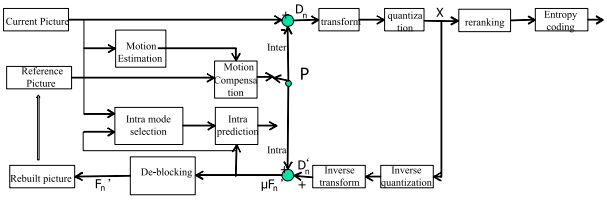

FIGURE 5. The H.264 Encoding framework.

coefficients are used to carry marked data. Since the smallest encoding unit is 4 × 4 block, AC coefficients are scanned in zigzag, then every three adjacent coefficients are grouped to be a triple. The modifications on these triples can be actualized based on the proposed 3D RDH in Section 2.

At the decoder side, the MVs hidden in the frames QDCT coefficients are extracted according to the proposed 3D RDH in Section 2. For the reversibility of data hiding, original video can be recovered after extraction. After that, if there are errors occurred through transmission, error MBs are concealed by replacing the matching MBs in reference frame according to the extracted MVs. Since data extraction process is actualized before de-quantization, the host MBs can be decoded without any extra distortion when there are no transmitting errors. Once the transmitting errors occur, the error concealment process is realized after the data extraction.

IV. EXPERIMENTAL RESULT

In this section, experiments are implemented to demonstrate the performance of the proposed scheme. The proposed scheme is capable of embedding the message into the QDCT coefficients using the proposed 3D RDH scheme method, and concealing the intra-frame error using the recovered MVs.

A. EXPERIMENTAL SETUP

In this Experiments, H.264, a highly practical encoder/decoder, is used to provide the compressed video samples. For each compressed video sample, the quantization parameter is set to be 28. In addition to the proposed scheme, [7] and [14] are implemented for comparison. In addition, to demonstrate the performance of the 3D RDH, [21] is used for comparing the 3D RDH performance. Six different video sequences(i.e., foreman, coastguard, hall, akiyo, grandma,silent) in QCIF format are used, and every 10 frames are considered as a GOP, the structure of GOP is *IPPP*, in which only the first frame in a GOP is encoded as an I-frame and the remaining frames are encoded as P-frames.

B. EMBEDDING DISTORTION

In this scheme, 3D RDH is used to embed the MVs into the QDCT coefficients. The goal of proposed RDH scheme is to improve embedding capacity and introduce low embedding distortion. However, since marked data are embedded into the host residual coefficients, it would cause difference between the host coefficients and marked coefficients. For the RDH algorithm, the host coefficients can be recovered completely from the embedding distortions if the video sequences are transmitted without any channel errors.

1) ECDR

Absolute embedding capacity and distortion ratio (ECDR) can be defined simply as

$$R_{ecdr} = C/D, \tag{20}$$

where C denotes the absolute embedding capacity, D denotes the absolute distortion, and both of them are calculated with the full embedding situation. In order to analyze the proposed 3D RDH performance better, the residual coefficient sets of the 1st, 2nd, 3rd,4rd case in Section 4 is defined as C_1, C_2, C_3. C_4 is defined in Eq.(25), C_5 denotes the original coefficient triples set of 5th and 6th case. The ECDR of the proposed 3D RDH is evaluated by comparing recent 3D RDH in [21]. Meanwhile, the embedding capacity of the proposed 3D RDH, and that in [21] are denoted as C_{pro}, C_{rec}, and the distortions in these schemes are denoted as D_{pro}, D_{rec}.

$$C_{pro} = \frac{11}{4}\sharp C_1 + \frac{3}{2}\sharp C_2 + \frac{9}{4}\sharp C_3 + \frac{3}{2}\sharp C_4 \tag{21}$$

$$C_{rec} = \frac{9}{4}\sharp C_1 + \sharp C_2 + 2\sharp C_3 + \sharp C_4 \tag{22}$$

$$D_{pro} = \frac{7}{8}\sharp C_1 + \sharp C_2 + 2\sharp C_3 + \frac{5}{4}\sharp C_4 + 2\sharp C_5 \tag{23}$$

$$\begin{aligned} D_{rec} = {} & \frac{3}{4}\sharp C_1 + \frac{3}{2}\sharp C_2 + \frac{5}{4}\sharp C_3 + \sharp\{(0,y,0)||y|>0\} \\ & + \frac{3}{2}\sharp\{(x,y,0)||x|>2,|y|>0\} + 2\sharp C_5 \\ & + 2\sharp\{(x,y,0)||x|=1,|y|>0\} + \frac{3}{2}\sharp\{(0,0,1)\} \end{aligned} \tag{24}$$

where $\sharp$ denotes the elements number in set. The embedding capacity and distortion difference are calculated as

$$C_{pro} - C_{rec} = \frac{1}{2}\sharp C_1 + \frac{1}{2}\sharp C_2 + \frac{1}{4}\sharp C_3 + \frac{1}{2}\sharp C_4 \tag{25}$$

$$\begin{aligned} D_{pro} - D_{rec} = {} & \frac{1}{8}\sharp C_1 - \frac{1}{2}\sharp C_2 + \frac{3}{4}\sharp C_3 - \frac{1}{4}\sharp\{(0,0,1)\} \\ & - \frac{1}{4}\sharp\{(x,y,0)||x|>2,|y|>0\} \\ & + \frac{1}{4}\sharp\{(0,y,0)||y|>0\} \end{aligned} \tag{26}$$

Eq. (25) indicates that the embedding capacity in proposed scheme is much more than that in the scheme [21] and Eq. (26) indicates that the distortion difference in the two schemes is decided by the elements number in C_1, C_2, C_3

TABLE 1. the embedding capacity and distortion comparison with [21].

	QP		18	20	22	24	26	28	30
foreman	EC	proposed	15802	16981	17939	18732	19444	19994	20484
		[21]	12792	13807	14633	15295	15905	16358	16762
	D	proposed	7329	7140	7023	6892	6859	6817	6795
		[21]	7051	7024	6819	6693	6510	6451	6309
hall	EC	proposed	16694	17893	18771	19822	20225	10577	20875
		[21]	13560	14595	15336	16204	16537	16828	17072
	D	proposed	6920	6816	6758	6787	6797	6816	6817
		[21]	7372	7048	6795	6528	6383	6280	6186
coastguard	EC	proposed	12586	14107	15405	16762	17900	18760	19624
		[21]	10034	11350	12459	13625	14591	15320	16041
	D	proposed	7996	7539	7190	7002	6857	6807	6758
		[21]	7480	7472	7411	7195	7043	6798	6589
grandma	EC	proposed	18781	19342	19730	20398	20679	20925	21254
		[21]	15301	15784	16114	16684	16909	17121	17396
	D	proposed	6748	6747	6721	6763	6786	6814	6852
		[21]	6871	6738	6557	6361	6276	6179	6100

and C_4. However, for video compressed standard, the number of the elements in these sets is mainly decided by quantization step. With the quantization step decreasing, coefficients with zero values decrease, and also the distortion difference may decrease. Generally, the quantization step is a number which can not make all the AC components are zeros. So the ECDR in the proposed scheme is more than that in the scheme [21] in great probability. Let $P(D_{pro}-D_{rec}>0)$ and $P(D_{pro}-D_{rec}<0)$ denote the probability of the case $D_{pro}-D_{rec}>0$ and $D_{pro}-D_{rec}<0$, then the relation of probability is described as

$$P(D_{pro}-D_{rec}>0)<P(D_{pro}-D_{rec}<0) \tag{27}$$

Assuming R_{ecdr}^{pro} and R_{ecdr}^{rec} denote the ECDR in the proposed scheme and in [21]. According to Eq.(25) and Eq.(26), R_{ecdr}^{pro} is greater than R_{ecdr}^{rec} in a higher probability, and it can be described as follows.

$$P(R_{ecdr}^{pro}=\frac{C_{pro}}{D_{pro}}>R_{ecdr}^{rec}=\frac{C_{rec}}{D_{rec}})>0.5 \tag{28}$$

To illustrate the ECDR of the two 3D RDH scheme, embedding capacity(EC) and the corresponding distortion of the 2nd frame in video sequence *foreman*, *hall*, *coastguard* and *grandma* are calculated in Table 1, in which 'EC' denote the embedding capacity and 'D' means distortion. It shows that with the quantization step (QP) increasing, the embedding capacity is increased too, and the distortion is decreased for the decreased shifting operations with lower QP. It also shows the proposed 3D RDH can provide more embedding space. Fig.6 shows the ECDR comparison of the ECDR in proposed 3D RDH is nearly two times as that in [21].

2) PSNRs OF MARKED FRAMES

Generally, at the decoder side, the quality of decoded frames without any other manipulations is the limitation of the concealed frames. If the peak signal to noise ratio (PSNR) values of marked frames are close to the limitations, the data hiding would have fewer influences on the marked video quality. However, α is also a key factor that impact the quality of

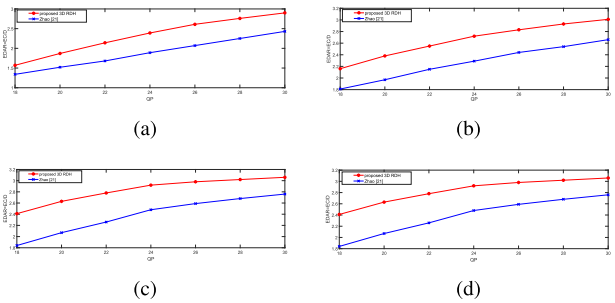

FIGURE 6. The EDAR of proposed 3D RDH comparison with [21]. (a) coastguard. (b) foreman. (c) hall. (d) grandma.

the marked frames. Higher α means more information is embedded into the frames and high distortion. To indicate the concealment performance with different α, the cases with $\alpha=1$ and $\alpha=5$ are compared with the limitation case. Fig.7 shows the PSNR values comparison of marked frames with the decoded frames in the proposed method, and it shows the PSNR values with $\alpha=1$ is near the limitation.

C. PERFORMANCE OF ERROR CONCEALMENT

1) ERROR CONCEALMENT PERFORMANCE COMPARISON

The error concealment performance is one of the most important features for this scheme. In mobile cloud environment, the packet lost rates (PLRs) can reflect all the channel states of the whole transition procedure. To simulate the transmission errors, different random intra-frame PLR are applied to each intra-frame, such as 0.05, 0.10, 0.15, 0.20 and 0.30. For every PLR, the performance is measured in terms of PSNR between original video sequence and concealed video sequence. The concealment performance comparison is taken with [7] and [14]. The PSNR performance comparisons of concealed frames are shown in Fig.8 and in both the cases $\alpha=1$ and $\alpha=5$ are considered. According to Fig.8, the error concealment performance in this proposed scheme is significantly better. Especially, with α increasing, the corrupted frames are fully concealed approximately. For the scheme

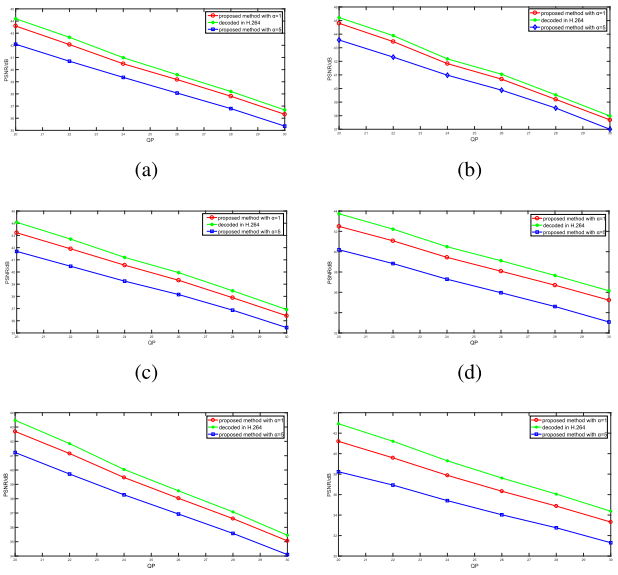

FIGURE 7. The PSNR values comparison of marked frame with the limitation. (a) grandma. (b) akiyo. (c) hall. (d) foreman. (e) silent. (f) coastguard.

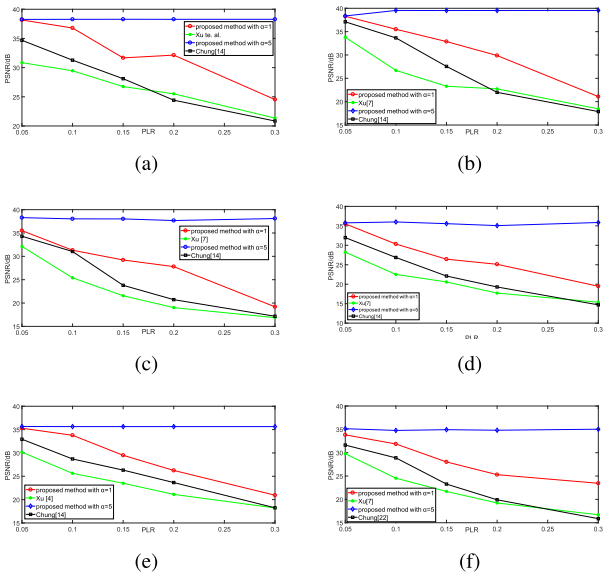

FIGURE 8. PSNR comparison of concealed frames. (a) grandma. (b) akiyo. (c) hall. (d) foreman. (e) silent. (f) coastguard.

in [7] and [14], correlation between the cover MB and its MV is stationary, and they can not resist continuous errors. In contrary, the embedding location of each MB is random in our proposed scheme, the corrupted MBs can be concealed in most cases.

Fig.9, Fig.10, and Fig.11 shows the visual quality of original frame, error frame, concealed frame in *coastguard*, *grandma* and *hall* sequences with PLR 0.2 and $\alpha = 1$ respectively. In this paper, all the errors caused by channel are occurred randomly and the corrupted frames are shown in Fig.9 (b), Fig.10 (b) and Fig.11 (b). The visual quality of the concealed frames is shown in Fig.9 (c), Fig.10 (c) and Fig.11(c).

FIGURE 9. Visual quality comparison for the *coastguard* sequence with PLR 0.2 and $\alpha = 1$. (a) original. (b) error. (c) conceaed.

FIGURE 10. Visual quality comparison for the *grandma* sequence with PLR 0.2 and $\alpha = 1$. (a) original. (b) error. (c) conceaed.

FIGURE 11. Visual quality comparison for the *coastguard* sequence with PLR 0.2 and $\alpha = 1$. (a) original. (b) error. (c) concealed.

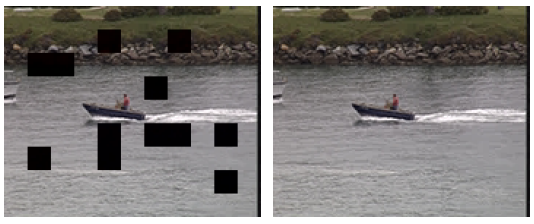

FIGURE 12. Visual quality comparison for the *coastguard* sequence with PLR 0.2 and $\alpha = 5$. (a) error. (b) conceaed.

FIGURE 13. Visual quality comparison for the *grandma* sequence with PLR 0.2 and $\alpha = 5$. (a) original. (b) error.

(a) (b)

FIGURE 14. Visual quality comparison for the *hall* sequence with PLR 0.2 and $\alpha = 5$. (a) original. (b) error.

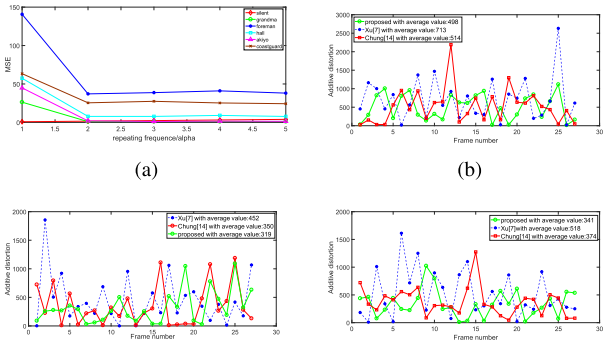

(a) (b) (c) (d)

FIGURE 15. MSE of concealed frames with different PLR. (a) additivedisconceal. (b) foreman. (c) hall. (d) coastguard.

Further, the visual quality of concealment performance is tested with $\alpha = 5$. Fig.12 (a), Fig.13 (a) and Fig.14 (a) show the error frames, and their original frames are the same as the Fig.9, Fig.10 and Fig.11. Fig.12 (b), Fig.13 (b) and Fig.14 (b) show the concealed frames with $\alpha = 5$, the concealed frame is similar in visual to the original frames.

2) MSE

PSNR denotes the peak SNR, it cannot reveal the distortion intuitively. Mean square error (MSE) is usually explored to capture the errors of every element, and it can reflect the comprehensive errors in a frame. For an error concealment scheme using RDH, the distortion may be generated both in the procedure of embedding and concealment. Without loss of generality, the original and the concealed frame with size $N_1 \times N_2$ are denoted as f_o and f_c, and the pixels in them are denoted as $P_{cij}, i = 1, 2, \cdots, N_1, j = 1, 2, \cdots, N_2$, and $P_{oij}, i = 1, 2, \cdots, N_1, j = 1, 2, \cdots, N_2$. The concealment distortion is defined as

$$D_{cd} = \frac{1}{N_1 \times N_2} \sum_{i,j} (P_{oij} - P_{cij})^2 \tag{29}$$

For the scheme in this paper, the quality of the concealed frames is controllable by tuning the number of duplicate copies. However, the concealment performance is mainly decided by the error concealment method. As we can see, the PSNR values and the visual quality can reflect the concealment performance, but they cannot reveal the detailed distortions in a frame. The MSE is the mean square value of distortions for all the pixels, also it can amplify the great distortion and reduce the low distortion. To explain the distortion of the concealment frames, Fig.15 shows the MSE of concealed frames with different α values and different videos. The MSE values of almost all the video sequences will achieve a steady performance with the repeating frequencies increasing. Also, for the test video *foreman*, *hall*, and *coastguard*, most of the MSE values are lower in the proposed scheme than those in [7] and [14]. Actually, since MVs are embedded randomly, the concealment performance of proposed scheme is better than that in [7] and [14] with high probability. In addition, under the hypothetical case that marked data is extracted correctly, the concealment performance is mainly decided by the correlation between the embedding locations and the error locations, and then, the random state of channel makes the concealment performance different every time.

V. CONCLUSION

For video communication, RTE under mobile cloud environment is a challenging problem. In this paper, a 3D RDH-based video error concealment technique is proposed for H.264 codec. At the encoder side, every three adjacent AC coefficients are counted to be a triple, and MVs are embedded in triples by shifting the triples. The proposed 3D RDH is utilized to embed the MVs into QDCT coefficients randomly. At the decoder side, MVs are extracted and recovered to conceal the corrupted MBs. Meanwhile, the marked data is controllable by tuning the number of duplicate copies, and then, both the concealment and embedding performance are adjustable correspondingly. The experimental results show that the scheme can benefit from creating duplicate copies and random embedding locations, and also the proposed high capacity 3D RDH. By using the proposed 3D RDH method, not only rich space are utilized to embed more marked data, but also it can improve the computational efficiency in cloud environment. How to take advantage of the 3D space characteristic to exploit a more suitable histogram modification should be researched in the future. Also, the error concealment scheme should be improved to achieve fewer embedding bits and better concealment performance for the mobile cloud environment.

REFERENCES

[1] T. Hobfeld, R. Schatz, M. Varela, and C. Timmerer, "Challenges of QoE management for cloud applications," *IEEE Commun. Mag.*, vol. 50, no. 4, pp. 28–36, Apr. 2012.
[2] M. Usman, X. He, K.-M. Lam, M. Xu, S. M. M. Bokhari, and J. Chen, "Frame interpolation for cloud-based mobile video streaming," *IEEE Trans. Multimedia*, vol. 18, no. 5, pp. 831–839, May 2016.
[3] A. Alasaad, K. Shafiee, H. M. Behairy, and V. C. M. Leung, "Innovative schemes for resource allocation in the cloud for media streaming applications," *IEEE Trans. Parallel Distrib. Syst.*, vol. 26, no. 4, pp. 1021–1033, Apr. 2015.
[4] Y. Chen, H. Wang, H. Wu, and X. Sun, "A video error concealment method using data hiding based on compressed sensing over lossy channel," *Telecommun. Syst.*, vol. 68, no. 2, pp. 337–349, 2018.

[5] J. Liu, G. Zhai, X. Yang, B. Yang, and L. Chen, "Spatial error concealment with an adaptive linear predictor," *IEEE Trans. Circuits Syst. Video Technol.*, vol. 25, no. 3, pp. 353–366, Mar. 2015.

[6] Y. Xu and Y. Zhou, "Adaptive temporal error concealment scheme for H.264/AVC video decoder," *IEEE Trans. Consum. Electron.*, vol. 54, no. 4, pp. 1846–1851, Nov. 2008.

[7] D. Xu and R. Wang, "Two-dimensional reversible data hiding-based approach for intra-frame error concealment in H.264/AVC," *Signal Process., Image Commun.*, vol. 47, pp. 369–379, Sep. 2016.

[8] C. B. Adsumilli, M. C. Q. Farias, S. K. Mitra, and M. Carli, "A robust error concealment technique using data hiding for image and video transmission over lossy channels," *IEEE Trans. Circuits Syst. Video Technol.*, vol. 15, no. 11, pp. 1394–1406, Nov. 2005.

[9] A. Yılmaz and A. A. Alatan, "Error detection and concealment for video transmission using information hiding," *Signal Process., Image Commun.*, vol. 23, no. 4, pp. 298–312, 2008.

[10] Y. Yao, W. Zhang, and N. Yu, "Adaptive video error concealment using reversible data hiding," in *Proc. MINES*, Nov. 2012, pp. 658–661.

[11] S. Chen and H. Leung, "A temporal approach for improving intra-frame concealment performance in H.264/AVC," *IEEE Trans. Circuits Syst. Video Technol.*, vol. 19, no. 3, pp. 422–426, Mar. 2009.

[12] Z. Ni, Y.-Q. Shi, N. Ansari, and W. Su, "Reversible data hiding," in *Proc. ISCS*, vol. 2, Bangkok, Thailand, May 2003, pp. 912–915.

[13] Z. Ni, Y.-Q. Shi, N. Ansari, and W. Su, "Reversible data hiding," *IEEE Trans. Circuits Syst. Video Technol.*, vol. 16, no. 3, pp. 354–362, Mar. 2006.

[14] K.-L. Chung, Y.-H. Huang, P.-C. Chang, and H.-Y. M. Liao, "Reversible data hiding-based approach for intra-frame error concealment in H.264/AVC," *IEEE Trans. Circuits Syst. Video Technol.*, vol. 20, no. 11, pp. 1643–1647, Nov. 2010.

[15] D. Xu, R. Wang, and Y. Q. Shi, "An improved reversible data hiding-based approach for intra-frame error concealment in H.264/AVC," *J. Vis. Commun. Image Represent.*, vol. 25, no. 2, pp. 410–422, 2014.

[16] K. Lin, J. Song, J. Luo, W. Ji, M. S. Hossain, and A. Ghoneim, "Green video transmission in the mobile cloud networks," *IEEE Trans. Circuits Syst. Video Technol.*, vol. 27, no. 1, pp. 159–169, Jan. 2017, doi: 10.1109/TCSVT.2016.2539618.

[17] Y. Tew and K. Wong, "An overview of information hiding in H.264/AVC compressed video," *IEEE Trans. Circuits Syst. Video Technol.*, vol. 24, no. 2, pp. 305–319, Feb. 2014.

[18] A. A. Muhit, M. R. Pickering, M. R. Frater, and J. F. Arnold, "Video coding using elastic motion model and larger blocks," *IEEE Trans. Circuits Syst. Video Technol.*, vol. 20, no. 5, pp. 661–672, May 2010.

[19] A. A. Muhit, M. R. Pickering, M. R. Frater, and J. F. Arnold, "Video coding using fast geometry-adaptive partitioning and an elastic motion model," *J. Vis. Commun. Image Represent.*, vol. 23, no. 1, pp. 31–41, 2012.

[20] J. Zhao, Z.-T. Li, and B. Feng, "A novel two-dimensional histogram modification for reversible data embedding into stereo H.264 video," *Multimedia Tools Appl.*, vol. 75, no. 10, pp. 5959–5980, 2016.

[21] J. Zhao and Z.-T. Li, "Three-dimensional histogram shifting for reversible data hiding," *Multimedia Syst.*, vol. 24, no. 1, pp. 95–109, 2018.

[22] B. Ou, X. Li, Y. Zhao, R. Ni, and Y.-Q. Shi, "Pairwise prediction-error expansion for efficient reversible data hiding," *IEEE Trans. Image Process.*, vol. 22, no. 12, pp. 5010–5021, Dec. 2013.

[23] S. Cai, X. Li, J. Liu, and Z. Guo, "A new reversible data hiding scheme exploiting high-dimensional prediction-error histogram," in *Proc. IEEE ICIP*, Sep. 2016, pp. 2732–2736.

[24] B. Ou, X. Li, W. Zhang, and Y. Zhao, "Improving pairwise PEE via hybrid-dimensional histogram generation and adaptive mapping selection," *IEEE Trans. Circuits. Syst. Video Technol.*, to be published, doi: 10.1109/TCSVT.2018.2859792.

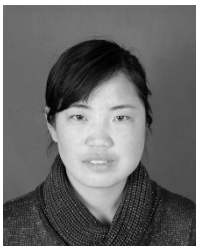

YAN LI CHEN is currently pursuing the Ph.D. degree with Southwest Jiaotong University, Chengdu, China. She is an Associate Professor with Tibet University, Lhasa, Tibet. Her research interests include information hiding, digital forensics, and video signal processing.

HONGXIA WANG received the B.S. degree from Hebei Normal University, Shijiazhuang, in 1996, and the M.S. and Ph.D. degrees from the University of Electronic Science and Technology of China, Chengdu, in 1999 and 2002, respectively. She pursued post-doctoral research work at Shanghai Jiao Tong University from 2002 to 2004, and she was a Visiting Scholar at Computer Science Department, Northern Kentucky University, USA, from 2013 to 2014. She is currently a Professor with the College of Cybersecurity, Sichuan University, Chengdu. She has published 100 peer research papers and wined 10 authorized patents. Her research interests include multimedia information security, information hiding, digital watermarking, and intelligent information processing.

YI HU received the Ph.D. degree in computer science from the University of Arkansas in 2006. He is a Professor of computer science at Northern Kentucky University, USA. His research concentrates on information assurance, database systems, data security, data mining, and trust management in cyberspace. He is also a CISSP and CEH.

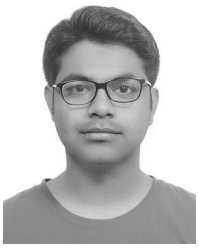

ASAD MALIK received the B.Sc. degree (Hons.) in computer application from Aligarh Muslim University in 2012 and the master's degree in computer application from Jamia Millia Islamia University, New Delhi, India, in 2015. He is currently pursuing the Ph.D. degree with the School of Information Science and Technology, Southwest Jiaotong University, Chengdu, China. His research interests include in the area of information security, reversible data hiding, and image processing.